DNA Repair 115 (2022) 103343

Contents lists available at ScienceDirect

DNA Repair

journal homepage: www.elsevier.com/locate/dnarepair

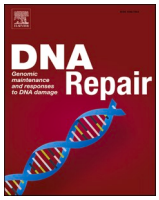

UBAP2/UBAP2L regulate UV-induced ubiquitylation of RNA polymerase II and are the human orthologues of yeast Def1

Anna E. Herlihy [a], Stefan Boeing [a], Juston C. Weems [b,c], Jane Walker [a], A. Barbara Dirac-Svejstrup [a,d], Michelle Harreman Lehner [a], Ronald C. Conaway [b,c], Joan W. Conaway [b,c], Jesper Q. Svejstrup [a,d,*]

[a] Mechanisms of Transcription Laboratory, The Francis Crick Institute, 1 Midland Road, London NW1 1AT, UK
[b] Department of Biochemistry & Molecular Biology, University of Kansas Medical Center, Kansas City, KS 66160, USA
[c] Stowers Institute for Medical Research, Kansas City, MO 64110, USA
[d] Department of Cellular and Molecular Medicine, Panum Institute, University of Copenhagen, Blegdamsvej 3B, Copenhagen N 2200, Denmark

ARTICLE INFO

Keywords:
UBAP2
UBAP2L
Def1
RNA polymerase II ubiquitylation
Transcription-coupled nucleotide excision repair
Ubiquitin

ABSTRACT

During transcription, RNA polymerase II (RNAPII) faces numerous obstacles, including DNA damage, which can lead to stalling or arrest. One mechanism to contend with this situation is ubiquitylation and degradation of the largest RNAPII subunit, RPB1 - the 'last resort' pathway. This conserved, multi-step pathway was first identified in yeast, and the functional human orthologues of all but one protein, RNAPII Degradation Factor 1 (Def1), have been discovered. Here we show that following UV-irradiation, human Ubiquitin-associated protein 2 (UBAP2) or its paralogue UBAP2-like (UBAP2L) are involved in the ubiquitylation and degradation of RNAPII through the recruitment of Elongin-Cul5 ubiquitin ligase. Together, our data indicate that UBAP2 and UBAP2L are the human orthologues of yeast Def1, and so identify the key missing proteins in the human last resort pathway.

1. Introduction

Cells have evolved a wide range of mechanisms to contend with transcription-obstructing DNA lesions, including the action of elongation factors and transcription-coupled nucleotide excision repair (TC-NER) [12,14,24]. Bulky DNA lesions caused by UV-irradiation are particularly problematic because they form a potent obstacle to RNAPII progress and thus potentially prevent all further transcription of the damaged gene [8,10,23]. At such lesions, ubiquitylation and degradation of stalled/arrested RNAPII can occur through the last resort pathway [14,42], which may allow access to the DNA lesion for repair proteins, such as those responsible for either TC-NER or global-genome NER (GG-NER). It is worth emphasizing that RNAPII ubiquitylation (and degradation) may also be important to deal with other kinds of transcription stress. For example, loss of elongation factor TFIIS results in RNAPII ubiquitylation as well, even in the absence of DNA damage [32,48]. Intriguingly, the NER pathways function in the context of a general cellular response to UV-irradiation, which includes genome-wide shutdown of transcription [14]. Recent work has shown that local ubiquitylation/degradation of RNAPII stalled at DNA lesions interconnects with this global transcription response through depletion of the global pool of RNAPII, enabling cells to shut down all transcription in response to high DNA damage loads [38].

The last resort pathway is highly regulated through the ubiquitin-proteasome system (UPS). It takes advantage of many UPS features, including mono-ubiquitylation that targets proteins for partial processing or recruitment, both degradative and non-degradative poly-ubiquitin chains, sequential ubiquitylation by distinct ubiquitin ligases (E3s) and extraction from chromatin by Cdc48/p97 [14,42]. The first E3 in the pathway, Rsp5 in yeast and NEDD4 in humans, mono-ubiquitylates RNAPII [2,5,16,34]. The second E3 is a Cullin/RING ubiquitin ligase (CRL) complex, Ela1/Elc1/Rbx1/Cul3 ($CRL3^{Elongin}$) in yeast and ElonginA/B/C/Rbx2/Cullin 5 ($CRL5^{Elongin}$) in human cells, which require prior RNAPII mono-ubiquitylation by Rsp5/NEDD4 [15], before poly-ubiquitylating the polymerase with K48-linked chains [15,29,30,45]. Such K48-linked poly-ubiquitylation targets RNAPII, specifically the largest subunit RPB1, for degradation by the proteasome after extraction by Cdc48 [27,39]. Several other E3 ligases have also been

* Corresponding author at: Department of Cellular and Molecular Medicine, Panum Institute, University of Copenhagen, Blegdamsvej 3B, Copenhagen N 2200, Denmark
E-mail address: jsvejstrup@sund.ku.dk (J.Q. Svejstrup).

https://doi.org/10.1016/j.dnarep.2022.103343
Received 24 February 2022; Received in revised form 25 April 2022; Accepted 9 May 2022
Available online 18 May 2022

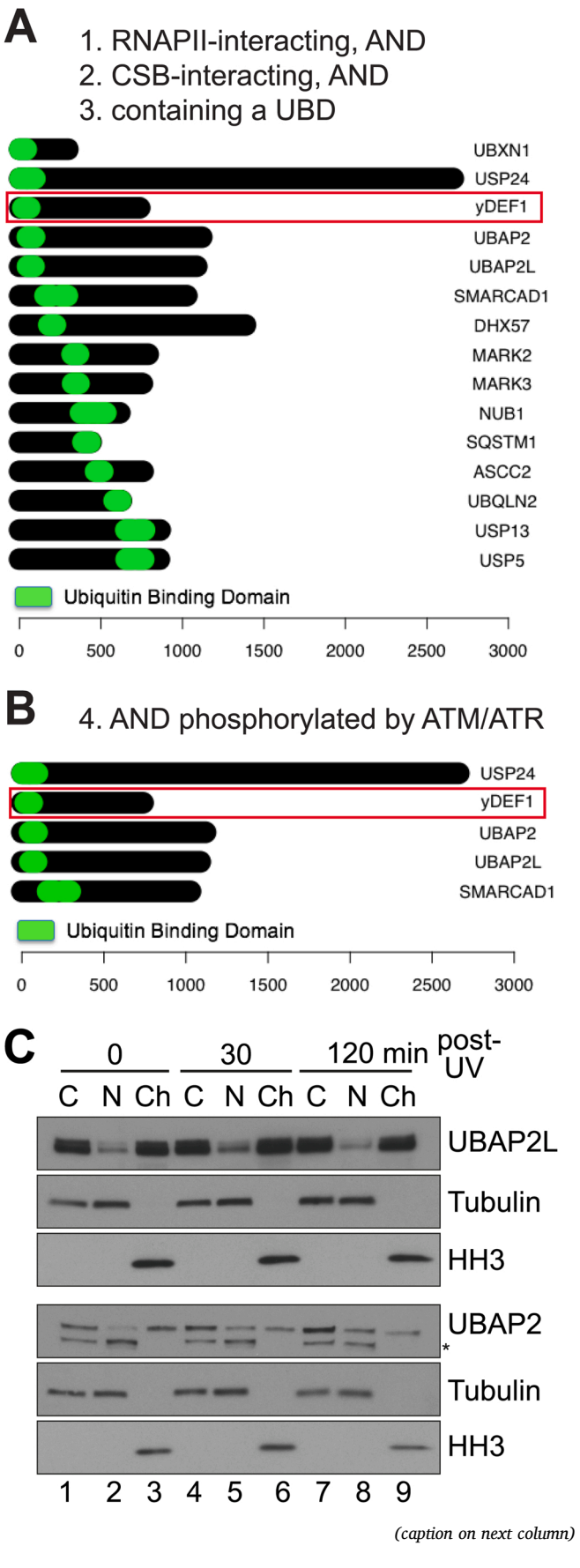

(caption on next column)

Fig. 1. UBAP2L and UBAP2 are candidates for a human orthologue of yeast Def1. **A.** Shortlist of proteins which satisfy the criteria shown. Green box indicates position of the UBD. Yeast Def1 included for comparison in red box. **B.** Shortlist of proteins from **A** that are also phosphorylated by ATM or ATR after DNA damage. **C.** Western blot of cellular fractions following 30 J/m^2 UV dose at the times shown in WT cells. 10 mg of cytoplasmic (C), nucleoplasm (N) or chromatin (Ch) fractions were loaded at each timepoint. HH3, histone H3. Representative Western of n = 3. Asterisk indicates unspecific band. See also Supplementary Fig. S1.

proposed for RPB1 poly-ubiquitylation [3,7,19,36].

Work in yeast has shown that Rsp5 also mono-ubiquitylates another protein as part of the damage response, namely Def1. This targets Def1 for processing ('protein clipping') by the proteasome, which in turn results in nuclear accumulation of this normally predominantly cytoplasmic protein. In the nucleus, Def1 binds RNAPII and acts as a bridge, recruiting CRL3^{Elongin} complex for RNAPII poly-ubiquitylation [28,43,44]. Although the discovery of Def1 was more than 20 years ago [44], and despite its importance in the response to UV damage, a human counterpart of Def1 has remained elusive.

Here, we identify UBAP2 and UBAP2L as human Def1 orthologues. In a manner akin to Def1 in yeast, these proteins are involved in the poly-ubiquitylation of RNAPII after UV-irradiation through the recruitment of the CRL5^{Elongin} complex to sites of DNA damage.

2. Results

2.1. UBAP2 and UBAP2L are candidate human orthologues of yeast Def1

Since the discovery of Def1 [44], we have repeatedly attempted to identify a human orthologue through sequence homology searching. However, probably due to its extended disordered regions, we have been unsuccessful with this approach. We therefore instead focused on functional homology - using different known characteristics of Def1 to identify human equivalents. Def1 is known to interact with both RNAPII [28] and Rad26 (yeast Cockayne syndrome B (CSB)) [44]. We therefore examined the numerous published and unpublished RNAPII and CSB pulldowns from human cells available in the lab, including those washed at low stringency (150 mM KCl) to select proteins that interact with *both* RNAPII and CSB. Importantly, Def1 contains a CUE domain, known to bind mono- and poly-ubiquitin [25,31,43]. We therefore also filtered the list of RNAPII- and CSB-interacting candidates for proteins that contain a ubiquitin-binding domain (UBD). This resulted in a candidate shortlist of 14 proteins (Fig. 1A). In addition, Def1 is phosphorylated in a Tel1/Mec1-dependent manner after DNA damage [33]. Therefore, we additionally filtered for human proteins phosphorylated in a manner dependent on ATM/ATR [22], the human orthologues of Tel1/Mec1. This further reduced the shortlist to four candidates (Fig. 1B). Among the proteins remaining on the list, USP24 is a ubiquitin protease and SMARCAD1 is a chromatin remodeler; these proteins are consequently highly unlikely to be the functional orthologues of Def1. The remaining candidates were the two closely related proteins, *ubiquitin-associated protein 2* (UBAP2) and *UBAP2-like* (UBAP2L), which share 43% identity. Like Def1, these proteins contain a UBD near their N-terminus. Def1 is an unusual protein, with extended disordered regions and a C-terminal half consisting of ~50% glutamine amino acids. Despite this, alignment of Def1 with UBAP2 and UBAP2L showed evidence of homology also beyond the CUE/UBA domains (Supplementary Fig. S1A).

Several other similarities between UBAP2, UBAP2L and Def1 were noted, *i.* UBAP2/2 L are both ubiquitylated following UV damage [11], like Def1 [43], *ii.* UBAP2/2 L contain PY motifs [17]. Such motifs are bound by WW domain proteins such as NEDD4, the human orthologue of Rsp5, which ubiquitylates Def1 in yeast [43]. Indeed, UBAP2L and NEDD4 interact [17], further supporting UBAP2/2 L as candidate Def1 orthologues.

Following UV-irradiation, Def1 undergoes proteasome-dependent

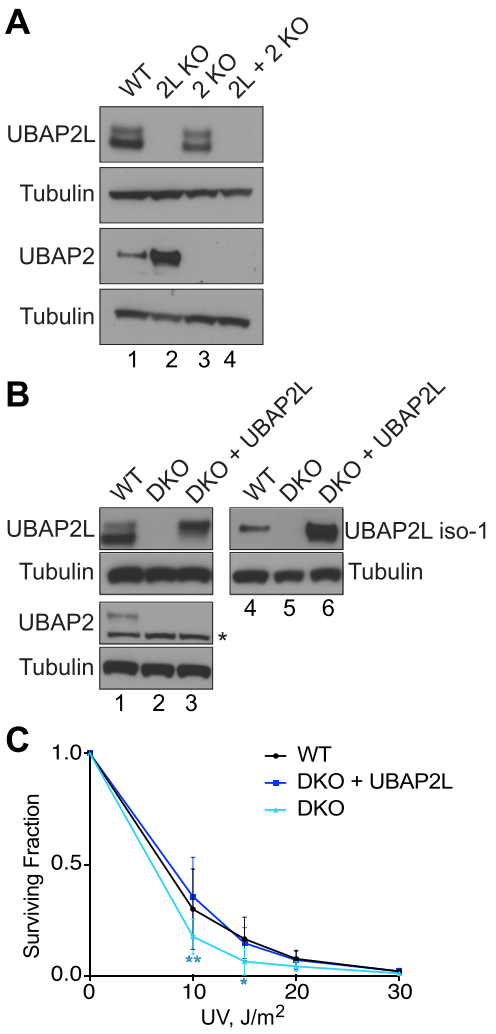

Fig. 2. UBAP2/2 L are involved in the UV damage response. **A.** Western blot showing UBAP2L and UBAP2 protein in WT, *UBAP2L* KO (2 L KO), *UBAP2* KO (2 KO), and *UBAP2/2 L* double knockout (2 L + 2 KO) cells. **B.** Western blot detecting UBAP2, UBAP2L or for panel on the right (lanes 4–6) using an antibody recognizing the C-terminal extension of UBAP2L isoform 1 in WT or *UBAP2/2 L* DKO cell lines. UBAP2L expression was maintained with Dox 1 μg/ml (DKO + UBAP2L) and dox removed for 4 days before cells were used as DKO in experiments. Asterisk indicates unspecific band. **C.** Quantification of colony assay showing UV-sensitivity. Colony numbers were normalized to untreated condition. 3 biological repeats, 2 technical replicates in each. Error bars show standard deviation (SD). Statistics: 2-way ANOVA with Dunnett's multiple comparisons to WT. *P < 0.05 ** P < 0.01. All other points, not significant (ns). See also Supplementary Fig. S1.

processing and only then accumulates in the nucleus [43]. We failed to uncover evidence for protein processing or nuclear accumulation of following UV-irradiation (data not shown); instead, UBAP2 and UBAP2L were detected in both the cytoplasmic and chromatin fractions before and after UV-irradiation (Fig. 1C).

2.2. *UBAP2/2 L are involved in the UV-damage response*

To investigate the cellular function of UBAP2/2 L, we used CRISPR/Cas9 technology to knock out *UBAP2, UBAP2L*, or both, in human MRC5 VA TetOn cells. Interestingly, when *UBAP2L* was knocked out (or knocked down) there was a consistent and marked increase in the levels of UBAP2 (Fig. 2A, lane 2; and data not shown). This suggests possible compensation between the genes/proteins, and so *UBAP2 UBAP2L* double knockout cell lines were used throughout this study. Moreover, we saw evidence of phenotypic changes in *UBAP2 UBAP2L* double knockout cell lines over time when grown in culture, indicative of adaptation occurring, possibly by mutation or dysregulation of compensatory factors. We therefore set out to avoid cells adapting to prolonged growth in the absence of *UBAP2/UBAP2L* by constructing double knockout cell lines but containing *UBAP2L* expressed from a doxycycline (Dox)-inducible promoter. This cell line was maintained in the presence of *UBAP2L* expression by Dox addition, so that the cells were only completely lacking UBAP2/2 L function during the experimental phase. UBAP2L isoform 1 contains an extended C terminal region and corresponds to the slower migrating band in Western blots (see for example Fig. 2B, lane 1). Indeed, an antibody directed against an epitope in this extended C terminal region recognizes only the upper band in wild type cells (Fig. 2B lane 4) as well as the Dox-induced UBAP2L Isoform 1 (lane 6) but not the lower band, which in wild type cells corresponds to shorter isoform 2 of UBAP2L. In case the extended C-terminal region contained domains that are important for the function of UBAP2L, the longer isoform 1 of UBAP2L was chosen for expression. The level of expression was adjusted so it resembled that of endogenous UBAP2L as much as possible. Upon Dox withdrawal, UBAP2L expression was at background levels after 4–5 days of growth (Supplementary Fig. S1B). Throughout this study, experiments were carried out with such generated cell lines, from which Dox had been withdrawn (labelled DKO) (Fig. 2B).

To initially assess if UBAP2/2 L are involved in the DNA damage response, we tested the effect of UV-irradiation through colony assays. As expected, in wild type cells the surviving fraction was reduced with increasing doses of UV. When DKO cells were maintained in the presence of Dox-induced UBAP2L (DKO + UBAP2L) there was no significant difference in UV sensitivity compared to wild type cells. However, when Doxycycline was removed and UBAP2L expression was lost, the DKO cells showed a significant increase in sensitivity to UV-irradiation (Fig. 2C). These data indicate a role for UBAP2/2 L in supporting cell growth and survival in response to UV damage.

2.3. *UBAP2/2 L are required for rapid poly-ubiquitylation of RNAPII following UV-irradiation*

Having found a first indication that UBAP2/2 L have a role in the UV damage response, we next tested whether they are also mechanistically similar to yeast Def1. In the last resort pathway, Def1 is required for poly-ubiquitylation of RNAPII (RPB1 subunit) after UV damage [28,43,44]. We tested the effect of UBAP2/2 L in human cells using DSK2 pulldown; this enriches for ubiquitylated proteins allowing for the detection of ubiquitylated RNAPII by Western blot analysis of RPB1, its largest subunit [2,37]. In wild type cells, 10 min after UV-irradiation a smear of poly-ubiquitylated RPB1 appears, and this increases further 30 min after irradiation (Fig. 3A). In the UBAP2/2 L DKO, such poly-ubiquitylation does still occur but is significantly delayed and reduced (Fig. 3A; quantified in Fig. 3B). This supports UBAP2/2 L having a role similar to Def1.

In these initial experiments, we detected RPB1 using the 4H8 antibody which preferentially recognizes the phosphorylated C-terminal domain (CTD) of RPB1. This represents the elongating form of RNAPII and is therefore also the form expected to primarily be targeted by the last resort pathway. However, similar results were seen whether using 4H8 or the D8L4Y antibody, which recognizes the N-terminal region of RPB1 and therefore all forms of RNAPII (Fig. 3C; quantified in Fig. 3D). We confirmed these observations in two further UBAP2/2 L double knockout clones. These were constructed (and maintained) with a CRISPR resistant, Dox-inducible, *shorter* isoform of UBAP2L (isoform 2), before CRISPR knock out of the endogenous *UBAP2* and *UBAP2L* genes. These *UBAP2 UBAP2L* DKO cell lines were again maintained with Dox-inducible expression of *UBAP2*L (in this case using the shorter *UBAP2L* isoform 2) to prevent adaptation. 4–5 days after Dox withdrawal, UBAP2L levels had reached background levels and experiments were

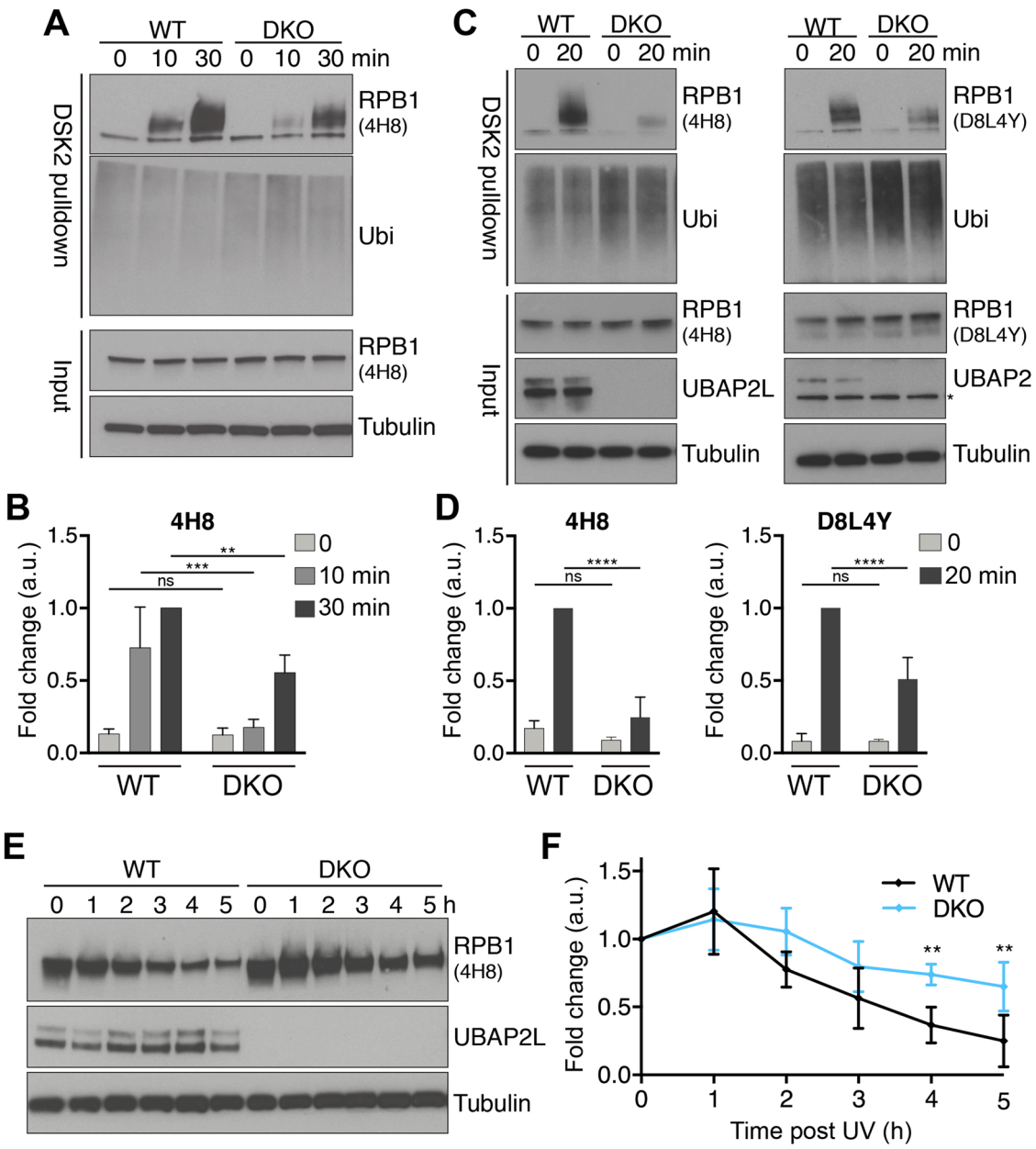

Fig. 3. UBAP2/2 L is required for efficient poly-ubiquitylation and degradation of RNAPII following UV-irradiation. **A.** DSK2 pulldown in WT and UBAP2/2 L DKO cell lines at times shown following 30 J/m^2 UV dose. **B.** Bar graph quantifying poly-ubiquitylation of RPB1 (4H8) from A, normalized to input, fold change over WT 30 m, n = 3, error bars show SD. Statistics: 2-way ANOVA with Sidak's multiple comparisons to WT. ** P < 0.01 *** P < 0.001. **C.** DSK2 pulldown in WT and UBAP2/2 L DKO cell lines at times shown following 30 J/m^2 UV dose. Asterisk indicates unspecific band. **D.** Bar graph quantifying poly-ubiquitylation of RPB1 from C, normalized to input, fold change over WT 20 m, n = 4, error bars show SD. Statistics as in B. **** P < 0.0001. **E.** Western blot showing time course following a 30 J/m^2 UV dose in WT and UBAP2/2 L DKO cells. **F.** Line graph quantifying RPB1 (4H8) levels from E, fold change over 0 h, n = 5, error bars show SD. Statistics: 2-way ANOVA with Sidak's multiple comparisons to WT. ** P < 0.01. See also Supplementary Fig. S2 and S3.

then performed in the absence of UBAP2 and UBAP2L. These clones also showed a significant reduction in poly-ubiquitylated RPB1 after UV-irradiation (Supplementary Fig. S2), further supporting the conclusions.

2.4. UBAP2/2 L deletion affects RNAPII degradation after UV-irradiation

We next asked whether the effect of UBAP2/2 L on RPB1 poly-ubiquitylation affects its degradation. Only a small proportion of RPB1 is ubiquitylated at any given time-point (cf. RPB1 inputs (1% loaded) and pulldown material (20% loaded) in Fig. 3A and C), and this portion is then degraded. As new damage-stalled polymerases are constantly targeted, the 'ubiquitylation-degradation' process repeats [2,42], so that there is slow but continuous depletion of RNAPII levels by the proteasome over the first 4–6 h after DNA damage (Fig. 3E; [42]). This underlies the shutdown of transcription of both damaged and undamaged genes [38]. As expected from the finding that DKO cells showed less ubiquitylation, RPB1 degradation following UV-irradiation was also slower in the DKO cells (Fig. 3E; quantified in Fig. 3F; see also Supplementary Fig. S3). Together, these data show that UBAP2/2 L affect ubiquitylation and thus degradation of RPB1.

2.5. UBAP2/2 L are essential for the recruitment of the CRL5^{Elongin} complex to sites of DNA damage

In yeast, poly-ubiquitylation of RNAPII involves Def1 recruiting the

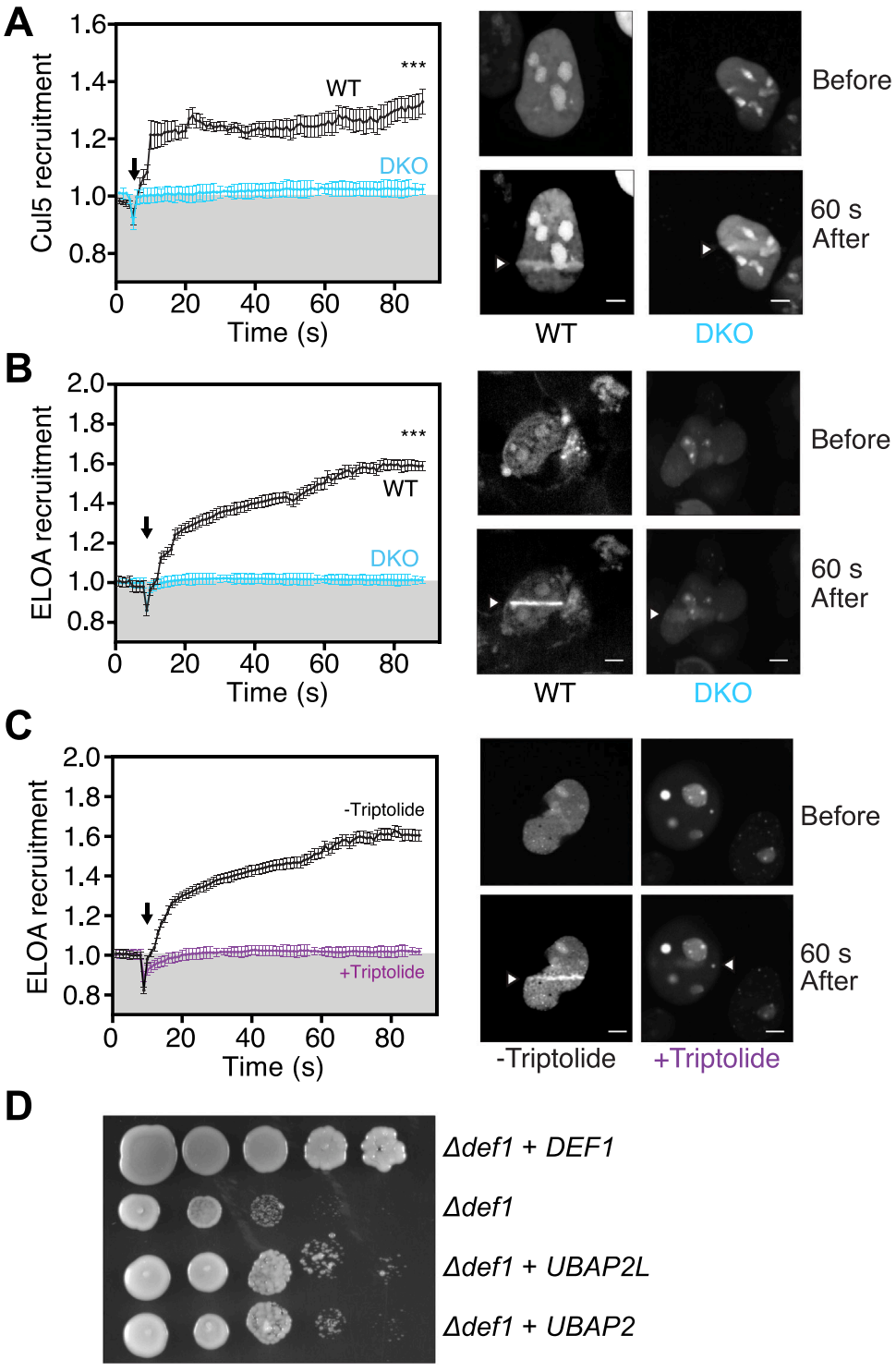

Fig. 4. UBAP2/2 L is required for recruitment of Elongin A and Cullin5 to sites of DNA damage. **A.** Recruitment of mCherry-Cul5 in WT and UBAP2/2 L DKO cell lines after laser micro-irradiation (indicated by black arrow). Left: Quantification, right: representative images with white arrows indicating stripe of micro-irradiation, scale bar 8 μm. Statistics: Unpaired t-test of last 10 time points. ***P < 0.001. **B.** As A., but recruitment of Halo-Elongin A (ELOA). **C.** As B., but for UBAP2/2 L DKO cell line with UBAP2L expression (Dox 1 μg/ml) with or without transcription inhibitor Triptolide – 125 nM for 16 h. **D.** Dilution series of yeast Δ*def1::URA* strain containing 2 μm plasmids expressing the genes shown.

Elongin/Cullin E3 complex to RNAPII [43]. We therefore investigated whether UBAP2/2 L might play a similar role in human cells, where Elongin A/B/C form a ubiquitin ligase complex with Cullin 5 and Rbx1 ($CRL5^{Elongin}$) [18], important for normal ubiquitylation of RPB1 after UV-irradiation [15,45]. For this purpose, we measured the recruitment of fluorescently tagged Cullin 5 and Elongin A to defined stripes of DNA damage generated by micro-irradiation (Fig. 4). In wild type cells, there was recruitment of Cullin 5 (Cul5; Fig. 4A) and Elongin A (ELOA, Fig. 4B) to sites of DNA damage, as previously demonstrated [40]. However, in the UBAP2/2 L DKO recruitment was dramatically reduced, demonstrating an important role for UBAP2/2 L in recruiting the $CRL5^{Elongin}$ complex to sites of DNA damage. Recruitment of the $CRL5^{Elongin}$ complex was transcription-dependent (Fig. 4C).

Together, the data above strongly support the idea that UBAP2 and UBAP2L are the human orthologues of yeast Def1. To test the extent to which UBAP2/UBAP2L function overlaps with that of Def1, we finally investigated whether expression of the human proteins might compensate for the absence of Def1 in yeast. Indeed, expression of *UBAP2* or *UBAP2L* was able to partially suppress the slow growth observed with yeast Δ*def1* cells (Fig. 4D). These results strongly indicate that UBAP2

and UBAP2L are indeed the human orthologues of yeast Def1.

3. Discussion

While this study identifies UBAP2 and UBAP2L as the human orthologues of yeast Def1, it also underscores interesting differences between the yeast and human last resort pathway. The most striking difference is that while *DEF1* deletion largely precludes RNAPII ubiquitylation and degradation in yeast [28,44], *UBAP2/2 L* double knockout has only relatively mild effects on RNAPII ubiquitylation and degradation in human cells. Interestingly, we previously uncovered a similar, incomplete dependence on the NEDD4 protein [2]. This difference is surprising given the experiments showing that recruitment of the $CRL5^{Elongin}$ complex to sites of DNA damage is dramatically affected by *UBAP2/2 L* deletion. The most logical explanation for these results is that the NEDD4-UBAP2/UBAP2L-$CRL5^{Elongin}$ axis, in contrast to the Rsp5-Def1-Elongin/Cullin axis in yeast, is not the only pathway to poly-ubiquitylate RNAPII after UV damage in human cells; there must be additional E3 ubiquitin ligases and response pathways that can compensate. Interestingly in this respect, previous reports have implicated a VHL-containing Cullin 2 E3 ligase complex ($CRL2^{VHL}$) in RNAPII ubiquitylation [19]. However, we did not see a noticeable further reduction in poly-ubiquitylation or degradation of RNAPII when *VHL* was knocked out in addition to UBAP2/2 L (data not shown). Other E3 ligase complexes have been connected to RNAPII ubiquitylation as well, including BRCA1 [36], $CRL4^{CSA}$ [7], and most recently a Cullin 3-based E3 [3]. Our results, both published [2,38] and unpublished, indicate that individual depletion of BRCA1 as well as any individual Cullin protein in human cells is insufficient to eliminate RNAPII ubiquitylation after DNA damage. By contrast, treatment with Neddylation inhibitor MLN4924 [35], which inactivates all Cullin E3 ligases, completely abolishes UV-induced RNAPII ubiquitylation [38]. Similarly, mutation of a single lysine in RPB1, lysine 1268, is sufficient to eliminate RNAPII poly-ubiquitylation as well [38]. Together, these results point to a complex and overlapping system of Cullin E3 ligases contributing to site-specific RNAPII ubiquitylation in human cells.

Beside its role in the DNA damage response, Def1 is involved in a range of other yeast processes [1]. UBAP2/2 L have not previously been implicated in the UV damage response or RNAPII ubiquitylation, but UBAP2L has roles in a number of different processes, including haemopoietic stem cell activity [6], chromosome alignment [20], epithelial to mesenchymal transition and tumor metastasis [4,46] and stress granules [9,21,47], indicating that UBAP2L, like yeast Def1, has numerous disparate roles. In all likelihood, both yeast Def1 and human UBAP2/2 L are multifunctional proteins with manifold roles as regulators of the ubiquitin proteasome system.

Acknowledgments

This work was supported by the Francis Crick Institute (FCI receives funding from Cancer Research UK [FC001166], the UK Medical Research Council [FC001166], and the Wellcome Trust [FC001166]), and by grants to J.Q.S. from the European Research Council (ERC Agreement 693327), the Novo Nordisk Foundation (Laureate grant, NNF19OC0055875), and the Danish National Research Foundation (Chair grant, DNRF153). We thank FCI's Cell Services and Proteomics for expert technical assistance; and Svejstrup lab members for discussions.

Author contributions

S.B. and J.Q.S. conceived the project. A.H. performed most of the experiments with contributions from S.B. (proteomics and bioinformatics for finding the Def1 homologue) J.W., (generation of human cell lines), J.C.W. (laser damage recruitment) as well as A.B.D.S and M.H.L. R.C.C, J.W.C. and J.Q.S. supervised the work. A.H. and J.Q.S. wrote the manuscript, with input from other authors.

Materials and methods

Experimental model and subject details

Cell lines and culture conditions

Cells were cultured in high glucose DMEM (Gibco, 41966–029) supplemented with 10% (v/v) FBS (Gibco, 10270–106), 100 U/ml penicillin, 100 μg/ml streptomycin, at 37 °C with 5% CO_2 and routinely passaged 2–3 times a week. All cell lines were confirmed to be mycoplasma-free. Cell lines containing a Doxycycline inducible construct were maintained in the presence of 1 μg/ml Doxycycline (Clontech, 8634–1), refreshed every 4–6 days. Cells grown in the absence of Doxycycline were washed twice in PBS and grown for 4–5 days in DMEM supplemented with 10% (v/v) Tet-free FBS (Clontech, 631106 or Biosera, FB-1001 T/500), 100 U/ml penicillin, 100 μg/ml streptomycin.

Yeast strains

Saccharomyces cerevisiae strains used in this study were grown and manipulated using standard techniques. All strains are in the W303 background. To obtain UBAP2L and UBAP2, RNeasy Mini Kit (Qiagen, 74104) purified RNA was used to generate random hexamer primed cDNA libraries using Taqman Reverse Transcription Reagents (Thermo Fisher Scientific, N8080234). Oligos were used to amplify UBAP2L and UBAP2 and the PCR product was cloned into the TOPO vector and sequenced. Strains JSY1226 and JSY1236 were created via recombination of UBAP2L and UBAP2 cDNA into the *DEF1* genomic locus of the Δ*def1::URA* strain (JSY568). Strains in which the *URA3* marker had been replaced by the desired cDNA were selected on 5-Fluroorotic acid and correct integration was checked by PCR analysis. JSY1190 serves as a control for experiments with these strains as the WT *DEF1* gene was integrated into Δ*def1::URA* (recreating a WT *DEF1* locus).

Method details

Plasmid construction

Plasmids for CRISPR knockouts were constructed as previously described [26] to insert gRNAs into plasmid PX458 to create PX458 plasmids targeting UBAP2L exon 4, UBAP2 exon 5, UBAP2L exon 2. Briefly, appropriate forward and reverse oligonucleotides were annealed and ligated into a *Bbs*I linearized PX458 (pSpCas9(BB)−2A-GFP). See resource table for oligonucleotide sequences used. Plasmids were sequenced after cloning and transformation.

Two doxycycline inducible UBAP2L expression plasmids were constructed. First the UBAP2L isoform 1 (longer) insert was amplified from UBAP2L in pcDNA5, cloned into a Zero Blunt TOPO vector (Thermo-Fisher Scientific) and ligated into the pTRE3G backbone with *Mlu*I and *Nhe*I. The UBAP2L isoform 2 (shorter) was constructed from the first plasmid using consecutive Q5 site directed mutagenesis (SDM) (NEB, E0554S) following manufacturer's instructions to switch the isoforms, insert a CRISPR resistant sequence over the gRNA site and convert two SNPs to their alternative forms (rs774812504 from T to C, rs17849745 from C to G).

Generation of stable cell lines

MRC5 VA TetON (WT) cells were transfected using Lipofectamine 3000 (Thermo Fisher Scientific, L3000001) following manufacturer's instructions with the relevant plasmids, as detailed below. For CRISPR knock outs: 72 h after transfection with pX458 plasmids single cells were sorted into 96 well plates with FACS and grown. Clones were expanded and checked for knock out by western blot and sequencing. For doxycycline-inducible expression: pTRE3G plasmids were co-

transfected with Hygromycin linear selection marker (Takara, 31625), after transfection: 24 h later media was changed, 48 h later cells were diluted, 72 h later 200 μg/ml Hygromycin was added. Clones were expanded and checked for Doxycycline inducible UBAP2L expression by western blot.

UBAP2L KO: Transfection with pX458_UBAP2L_exon4 to knock out *UBAP2L*.

UBAP2 KO: Transfection with pX458_UBAP2_exon5 to knock out *UBAP2*.

UBAP2/2 L KO: Co-transfection with pX458_UBAP2_exon5 and pX458_UBAP2L_exon4 to knock out *UBAP2* and *UBAP2L*.

DKO: Co-transfection with pX458_UBAP2_exon5 and pX458_UBAP2L_exon4 to knock out *UBAP2* and *UBAP2L*, followed by transfection with pTRE3G_UBAP2L_isoform1 to allow Doxycycline-inducible expression of UBAP2L isoform 1. These cells were maintained in the presence of Doxycycline-induced UBAP2L (DKO + UBAP2L). Cells were used for experiments as DKO 4–5 days after Dox withdrawal when UBAP2L expression was at background levels.

DKO clF2 and DKO clH2: Transfection with pTRE3G_UBAP2L_isoform2_CRISPR_resistant to allow Doxycycline-inducible expression of CRISPR-resistant UBAP2L isoform 2, followed by co-transfection with pX458_UBAP2_exon5 and pX458_UBAP2L_exon2 to knock out *UBAP2* and *UBAP2L*. These cells were maintained in the presence of Doxycycline-induced *UBAP2L*. Cells were used for experiments as DKO 4–5 days after Dox withdrawal when UBAP2L expression was at background levels.

UV-irradiation

UV-irradiation was performed as previously described [37]. Media was removed, cells were irradiated with either Stratalinker (Stratagene) or a custom-made UV conveyor belt and the same media replaced. UVC was used and doses were monitored using a UV meter (Progen Scientific) in all experiments.

Cellular Fractionation

Cells were plated in 15 cm plates to be around 80% confluent the following day when they were UV irradiated at 30 J/m^2. At time points indicated cells were washed with ice cold PBS, scraped into an Eppendorf tube in ice cold PBS and pelleted at 300 g, 4 °C, 5 min. Cellular fractionation was carried out as previously described [13]. All buffers contained cOmplete protease inhibitor (Sigma, 5056489001) and phosSTOP phosphatase inhibitor (Sigma, 4906837001). Pellets were resuspended in 500 μl hypotonic buffer (10 mM HEPES pH 7.5, 10 mM KCl, 1.5 mM $MgCl_2$) and incubated on ice for 15 min, homogenized with 20 strokes using a loose pestle and spun at 3,000 g, 4 °C, 15 min. Supernatant was taken as the cytoplasmic extract and corrected to 10% (v/v) glycerol, 3 mM EDTA, 0.05% (v/v) NP-40, 150 mM NaCl. The remaining nuclear pellets were resuspended in 500 μl nucleoplasmic extraction buffer (20 mM HEPES pH 7.5, 1.5 mM $MgCl_2$, 150 mM Potassium Acetate, 10% v/v Glycerol, 0,05% (v/v) NP-40) and incubated on ice for 20 min, then spun at 20,000 g, 4 °C, 20 min to pellet chromatin. Supernatant was taken as the Nucleoplasmic fraction. The remaining chromatin pellets were resuspended in 200 μl chromatin digestion buffer (20 mM HEPES pH 7.9, 1.5 mM $MgCl_2$, 150 mM NaCl, 10% (v/v) Glycerol, 0.05% (v/v) NP-40, 1:1000 BaseMuncher (Abcam, ab270049)) and incubated for 1 h, 4 °C, rotating, then spun at 20,000 g, 4 °C, 20 min, supernatant was taken as the low salt chromatin fraction. Pellets were resuspended in 120 μl high salt chromatin extraction buffer (20 mM HEPES pH 7.9, 500 mM NaCl, 3 mM EDTA, 1.5 mM $MgCl_2$, 10% v/v Glycerol, 0.05% (v/v) NP-40) and incubated on ice for 20 min. 280 μl high salt dilution buffer (20 mM HEPES pH 7.9, 3 mM EDTA, 1.5 mM $MgCl_2$, 10% (v/v) Glycerol, 0.05% (v/v) NP-40) was added and samples spun at 20,000 g, 4 °C, 15 min. Supernatant was pooled with low salt chromatin fraction to form the chromatin fraction. Protein concentration was measured (Protein Assay Dye Reagent, Bio-Rad, 5000006) in a plate reader.

Western blotting

Whole cell extracts were collected from 6 well plates by washing with PBS, adding 100 μl RIPA buffer (TrisHCL pH 7.5 50 mM, NaCl 150 mM, NP40 1% (v/v), Sodium Deoxycholate 0.5% (w/v), SDS 0.1%) containing cOmplete protease inhibitor (Sigma, 5056489001) and phosSTOP phosphatase inhibitor (Sigma, 4906837001), incubating on ice for 2 min and then scraping to Eppendorf tubes. Samples were sonicated in a Bioruptor water bath sonicator (Diagenode) on high 30 s ON/30 s OFF for 5 min. Samples were then spun at 20,000 g, 4 °C, 5 min and supernatant taken. Protein concentration was measured (Protein Assay Dye Reagent, Bio-Rad, 5000006) in a plate reader. 10 or 15 μg protein/lane was separated on 4–15% Criterion TGX (Bio-Rad, 5671084) or NuPAGE 3 to 8% Tris-Acetate (Thermo Fisher Scientific, WG1602) gels and transferred to nitrocellulose (GE Healthcare Life Sciences, 10600002). Membranes were blocked in 5% (w/v) skimmed milk in PBS-T (PBS, 0.2% (v/v) Tween20) for 1 h at room temperature and incubated in primary antibody in 5% (w/v) skimmed milk in PBS-T overnight at 4 °C. Membranes were washed 3 times in PBS-T, incubated for 1 h at room temperature in HRP-conjugated secondary antibodies (anti-mouse, Santa Cruz, sc516102 or anti-rabbit, Jackson, 711035152) and visualized with SuperSignal West Pico PLUS Chemiluminescent Substrate (Thermo Fisher Scientific, 34580). Supplementary Figs. S1B and S3C used Immobilon-FL membrane (Merck, IPFL00010), were blocked in Intercept blocking buffer (Licor, 927–70001), fluorescent secondary antibodies (Invitrogen, anti-mouse Alexa Fluor 680, A10038, anti-rabbit Alexa Fluor 680 or anti-rabbit Alexa Fluor Plus 800) and were visualized on LiCor Odyssey CLx.

Colony assays

Cells were seeded in 6-well plates (500 cells/well for untreated, 2,000–5,000 cells/well for UV treated). The following day media was removed and cells irradiated with varying UV doses and the same media replaced. Colonies were allowed to grow for 2 weeks before being washed carefully with PBS and fixed with 3.7% Formaldehyde for 20 m and washed with water. Colonies were stained with 0.1% (w/v) crystal violet solution, scanned and colonies counted manually.

Preparing GST-Dsk2 Affinity Resin

GST-Dsk2 affinity resin was prepared as previously described [37]. One Shot BL21 (DE3) Star bacteria were transformed with pGEX3-Dsk2 plasmid according to manufacturer's instructions. 10 ml overnight culture was used to inoculate a 250 ml culture grown to $OD_{600} = 0.6$, all at 37 °C in LB with 100 μg/ml Ampicillin (VWR, 171254–25) and shaking. Expression was induced with 1 mM IPTG and bacteria grown at 30 °C with shaking for 4 h, cells were then pelleted and snap frozen in liquid nitrogen. The pellet was resuspended in 40 ml PBS with protease inhibitors (2.2 mM PMSF, 2 mM Benzamidine HCL, 2 μM Leupeptin, 1 μg/ml Pep statin A) and sonicated (Branson Digital Sonifer 250) at 30% output for 15 s ON/30 s OFF pulses for a total of 10 min ON time on ice. Triton X100 was added to 0.5%, mixed gently and incubated on ice for 30 min. Following a 12,000 g, 4 °C, 10 min spin the supernatant (lysate) was taken and DTT added to 2 mM final concentration. 1 ml Glutathione Sepharose 4B Beads (Sigma, GE17–0756-01) were spun at 700 g, washed twice in PBS, added to the lysate and incubated at 4 °C with rotation for 4 h. Beads were then spun at 700 g, washed for 5 min twice with ice cold PBS + 0.1% Triton X100 then once with ice cold PBS. Finally 1 ml GST-DSK2 affinity resin was resuspended in 3 ml PBS and stored at 4 °C before use.

DSK2 ubiquitin pulldown

Cells were plated in 1×10 cm dish per condition such that cells were around 80% confluent the following day for UV-irradiation. Following UV-irradiation, at the indicated times media was removed, cells washed with PBS alone or PBS containing 2 mM NEM (200 mM stock in ethanol made fresh). 800 µl TENT buffer (50 mM TrisHCL pH7.4, 2 mM EDTA, 150 mM NaCl, 1% Triton X100) containing 2 mM NEM (200 mM stock in ethanol made fresh) and protease inhibitors (2.2 mM PMSF, 2 mM Benzamidine HCL, 2 µM Leupeptin, 1 µg/ml Pep statin A) was added and incubated for 5 min, then scraped into an Eppendorf or falcon. Samples were incubated on ice for 20 min then sonicated, Branson Digital Sonifer 250 at 20% output for 10 s or Bioruptor water bath sonicator (Diagenode) on high 30 s ON/ 30 s OFF for 7 min. $MgCl_2$ to 3 mM and BaseMuncher 1:1,000 (Expedeon, BM0100) were added to each sample and incubated for 1 h at 4 °C with rotation. Samples were spun at 20,000 g, 4 °C, 5 min and the supernatant taken.

Protein concentration was measured (Protein Assay Dye Reagent, Bio-Rad, 5000006) and each sample adjusted with TENT buffer to 750 µl at 1 mg/ml, a 1% input was taken and boiled with Sample buffer. 120 µl per sample of bead suspension (30 µl packed bead volume, GST-DSK2 affinity resin) was spun down at 700 g and resuspended in equivalent volume of TENT buffer. 120 µl was added to each sample and rotated overnight at 4 °C. Beads were spun down at 700 g, washed with 5 min, 4 °C, rotating incubations twice in TENT buffer and once in PBS. 50 µl 1x Sample Buffer was added and the sample boiled for 2 min. 1% input and 20% sample were run on a 4–15% Criterion TGX gel (Bio-Rad, 5671084) and normal Western blotting procedure followed.

Protein recruitment to sites of DNA damage

Cells were plated in MatTek dishes (35 mm, No. 2 14 mm diameter glass) at a density of 2×10^6 per dish in media containing 200 µg/ml G418. Cells were transfected with 400 ng of either Halo-Elongin A or mCherry-CUL5 plasmid DNA [41] using FugeneHD (Promega), 24 h prior to imaging. To label Halo-tagged Elongin A with rhodamine 110 in living cells, HaloTag ®R110Direct™ ligand was added to a final concentration of 100 nM, and cells were allowed to incubate overnight without washing as directed in the manufacturer's protocol. 30 min prior to imaging, culture medium was replaced with phenol-red free medium containing the same additives plus 1 µg/ml Hoechst 33258 to label nuclei and sensitize cells to UV-irradiation.

UV-microirradiation was performed by subjecting cell nuclei to laser micro-irradiation in a 200 × 3 pixel (34 × 0.51 µm) stripe. Micro-irradiation was performed with 100% 405 nm laser power and cells were exposed to 500–700 µW for approximately 3 s (40 iterations). Normal cell and nuclear morphology were preserved over the time scale of the experiment. Micro-irradiation and imaging were performed on a Perkin Elmer UltraVIEW VoX spinning disk microscope, which included a Yokagawa CSU-X11 spinning disk, an ORCA-R2 camera (Hamamatsu), and a Perkin Elmer PhotoKinesis accessory. The microscope base was a Carl Zeiss Axiovert 200 M equipped with a 40 × 1.3 NA Plan-Apochromat objective and a 37 °C, 5% CO_2 incubator (Solent Scientific). R110Direct labeled Halo-ELOA was excited with the 488 nm laser and imaged with a 500–550 emission filter. mCherry was excited with the 561-nm laser and imaged through a 415–475-nm, 580–650-nm multiband emission filter. Hoechst was excited with the 405-nm laser and imaged through a 415–475-nm, 580–650-nm multiband emission filter. Laser power and exposure time were adjusted before-hand to maximize image quality and minimize photobleaching; absence of significant photobleaching was confirmed by observing unperturbed cells in the acquisition field of view.

Yeast dilution series growth assays

Overnight yeast cultures were diluted to early logarithmic phase and grown for approximately 4 h. Tenfold serial dilutions were made and spotted on YPD agar plates and incubated at 30 °C for 2–3 days. After growth, the plates were photographed using a GelDoc XR (Bio-Rad).

Quantification and statistical analysis

Details of statistical tests used and numbers of replicates are detailed in the relevant figure legend. Throughout * $P < 0.05$, ** $P < 0.01$, *** $P < 0.001$, **** $P < 0.0001$. Statistical analysis was carried out in Prism 7 software. Quantification of western blots was carried out in ImageStudioLite software.

Appendix A. Supporting information

Supplementary data associated with this article can be found in the online version at doi:10.1016/j.dnarep.2022.103343.

References

[1] O.T. Akinniyi, J.C. Reese, DEF1: Much more than an RNA polymerase degradation factor, DNA Repair (Amst.) 107 (2021), 103202.
[2] R. Anindya, O. Aygun, J.Q. Svejstrup, Damage-induced ubiquitylation of human RNA Polymerase II by the ubiquitin ligase nedd4, but not cockayne syndrome proteins or BRCA1, Mol. Cell 28 (2007) 386–397.
[3] Y. Aoi, Y.H. Takahashi, A.P. Shah, M. Iwanaszko, E.J. Rendleman, N.H. Khan, B. K. Cho, Y.A. Goo, S. Ganesan, N.L. Kelleher, et al., SPT5 stabilization of promoter-proximal RNA Polymerase II, Mol. Cell 81 (4413–4424) (2021), e4415.
[4] R. Aucagne, S. Girard, N. Mayotte, B. Lehnertz, S. Lopes-Paciencia, P. Gendron, G. Boucher, J. Chagraoui, G. Sauvageau, UBAP2L is amplified in a large subset of human lung adenocarcinoma and is critical for epithelial lung cell identity and tumor metastasis, FASEB J. 31 (2017) 5012–5018.
[5] S.L. Beaudenon, M.R. Huacani, G. Wang, D.P. McDonnell, J.M. Huibregtse, Rsp5 ubiquitin-protein ligase mediates DNA damage-induced degradation of the large subunit of RNA polymerase II in Saccharomyces cerevisiae, Mol. Cell Biol. 19 (1999) 6972–6979.
[6] M.E. Bordeleau, R. Aucagne, J. Chagraoui, S. Girard, N. Mayotte, E. Bonneil, P. Thibault, C. Pabst, A. Bergeron, F. Barabe, et al., UBAP2L is a novel BMI1-interacting protein essential for hematopoietic stem cell activity, Blood 124 (2014) 2362–2369.
[7] D.B. Bregman, R. Halaban, A.Jv Gool, K.A. Henning, E.C. Friedberg, S.L. Warren, UV-induced ubiquitination of RNA polymerase II: a novel modification deficient in Cockayne syndrome cells, Proc. Natl. Acad. Sci. USA 93 (1996) 11586–11590.
[8] F. Brueckner, U. Hennecke, T. Carell, P. Cramer, CPD damage recognition by transcribing RNA polymerase II, Science 315 (2007) 859–862.
[9] L. Cirillo, A. Cieren, S. Barbieri, A. Khong, F. Schwager, R. Parker, M. Gotta, UBAP2L forms distinct cores that act in nucleating stress granules upstream of G3BP1, Curr. Biol. 30 (698–707) (2020), e696.
[10] B.A. Donahue, S. Yin, J.S. Taylor, D. Reines, P.C. Hanawalt, Transcript cleavage by RNA polymerase II arrested by a cyclobutane pyrimidine dimer in the DNA template, Proc. Natl. Acad. Sci. USA 91 (1994) 8502–8506.
[11] A.E. Elia, A.P. Boardman, D.C. Wang, E.L. Huttlin, R.A. Everley, N. Dephoure, C. Zhou, I. Koren, S.P. Gygi, S.J. Elledge, Quantitative Proteomic Atlas of Ubiquitination and Acetylation in the DNA Damage Response, Mol. Cell 59 (2015) 867–881.
[12] L. Gaul, J.Q. Svejstrup, Transcription-coupled repair and the transcriptional response to UV-Irradiation, DNA Repair (Amst.) 107 (2021), 103208.
[13] L.H. Gregersen, R. Mitter, A.P. Ugalde, T. Nojima, N.J. Proudfoot, R. Agami, A. Stewart, J.Q. Svejstrup, SCAF4 and SCAF8, mRNA anti-terminator proteins, Cell 177 (1797–1813) (2019), e1718.
[14] L.H. Gregersen, J.Q. Svejstrup, The cellular response to transcription-Blocking DNA damage, Trends Biochem Sci. 43 (2018) 327–341.
[15] M. Harreman, M. Taschner, S. Sigurdsson, R. Anindya, J. Reid, B. Somesh, S. E. Kong, C.A. Banks, R.C. Conaway, J.W. Conaway, et al., Distinct ubiquitin ligases act sequentially for RNA polymerase II polyubiquitylation, Proc. Natl. Acad. Sci. USA 106 (2009) 20705–20710.
[16] J.M. Huibregtse, J.C. Yang, S.L. Beaudenon, The large subunit of RNA polymerase II is a substrate of the Rsp5 ubiquitin-protein ligase, Proc. Natl. Acad. Sci. USA 94 (1997) 3656–3661.
[17] R.J. Ingham, K. Colwill, C. Howard, S. Dettwiler, C.S. Lim, J. Yu, K. Hersi, J. Raaijmakers, G. Gish, G. Mbamalu, et al., WW domains provide a platform for the assembly of multiprotein networks, Mol. Cell Biol. 25 (2005) 7092–7106.
[18] T. Kamura, D. Burian, Q. Yan, S.L. Schmidt, W.S. Lane, E. Querido, P.E. Branton, A. Shilatifard, R.C. Conaway, J.W. Conaway, Muf1, a novel Elongin BC-interacting leucine-rich repeat protein that can assemble with Cul5 and Rbx1 to reconstitute a ubiquitin ligase, J. Biol. Chem. 276 (2001) 29748–29753.
[19] A.V. Kuznetsova, J. Meller, P.O. Schnell, J.A. Nash, M.L. Ignacak, Y. Sanchez, J. W. Conaway, R.C. Conaway, M.F. Czyzyk-Krzeska, von Hippel-Lindau protein binds hyperphosphorylated large subunit of RNA polymerase II through a proline hydroxylation motif and targets it for ubiquitination, Proc. Natl. Acad. Sci. USA 100 (2003) 2706–2711.

[20] M. Maeda, H. Hasegawa, M. Sugiyama, T. Hyodo, S. Ito, D. Chen, E. Asano, A. Masuda, Y. Hasegawa, M. Hamaguchi, et al., Arginine methylation of ubiquitin-associated protein 2-like is required for the accurate distribution of chromosomes, FASEB J. 30 (2016) 312–323.
[21] S. Markmiller, S. Soltanieh, K.L. Server, R. Mak, W. Jin, M.Y. Fang, E.C. Luo, F. Krach, D. Yang, A. Sen, et al., Context-dependent and disease-specific diversity in protein interactions within stress granules, Cell 172 (590–604) (2018), e513.
[22] S. Matsuoka, B.A. Ballif, A. Smogorzewska, E.R. McDonald 3rd, K.E. Hurov, J. Luo, C.E. Bakalarski, Z. Zhao, N. Solimini, Y. Lerenthal, et al., ATM and ATR substrate analysis reveals extensive protein networks responsive to DNA damage, Science 316 (2007) 1160–1166.
[23] J.S. Mei Kwei, I. Kuraoka, K. Horibata, M. Ubukata, E. Kobatake, S. Iwai, H. Handa, K. Tanaka, Blockage of RNA polymerase II at a cyclobutane pyrimidine dimer and 6-4 photoproduct, Biochem Biophys. Res Commun. 320 (2004) 1133–1138.
[24] M. Noe Gonzalez, D. Blears, J.Q. Svejstrup, Causes and consequences of RNA polymerase II stalling during transcript elongation, Nat. Rev. Mol. Cell Biol. 22 (2021) 3–21.
[25] C.P. Ponting, Novel domains and orthologues of eukaryotic transcription elongation factors, Nucleic Acids Res 30 (2002) 3643–3652.
[26] F.A. Ran, P.D. Hsu, J. Wright, V. Agarwala, D.A. Scott, F. Zhang, Genome engineering using the CRISPR-Cas9 system, Nat. Protoc. 8 (2013) 2281–2308.
[27] J.N. Ratner, B. Balasubramanian, J. Corden, S.L. Warren, D.B. Bregman, Ultraviolet radiation-induced ubiquitination and proteasomal degradation of the large subunit of RNA polymerase II. Implications for transcription-coupled DNA repair, J. Biol. Chem. 273 (1998) 5184–5189.
[28] J. Reid, J.Q. Svejstrup, DNA damage-induced Def1-RNA polymerase II interaction and Def1 requirement for polymerase ubiquitylation in vitro, J. Biol. Chem. 279 (2004) 29875–29878.
[29] B. Ribar, L. Prakash, S. Prakash, Requirement of ELC1 for RNA polymerase II polyubiquitylation and degradation in response to DNA damage in Saccharomyces cerevisiae, Mol. Cell Biol. 26 (2006) 3999–4005.
[30] B. Ribar, L. Prakash, S. Prakash, ELA1 and CUL3 are required along with ELC1 for RNA polymerase II polyubiquitylation and degradation in DNA-damaged yeast cells, Mol. Cell Biol. 27 (2007) 3211–3216.
[31] S.C. Shih, G. Prag, S.A. Francis, M.A. Sutanto, J.H. Hurley, L. Hicke, A ubiquitin-binding motif required for intramolecular monoubiquitylation, the CUE domain, Embo J. 22 (2003) 1273–1281.
[32] S. Sigurdsson, A.B. Dirac-Svejstrup, J.Q. Svejstrup, Evidence that transcript cleavage is essential for RNA polymerase II transcription and cell viability, Mol. Cell 38 (2010) 202–210.
[33] M.B. Smolka, C.P. Albuquerque, S.H. Chen, H. Zhou, Proteome-wide identification of in vivo targets of DNA damage checkpoint kinases, Proc. Natl. Acad. Sci. USA 104 (2007) 10364–10369.
[34] B.P. Somesh, J. Reid, W.-F. Liu, T.M.M. Søgaard, H. Erdjument-Bromage, P. Tempst, J.Q. Svejstrup, Multiple mechanisms confining RNA Polymerase II ubiquitylation to polymerases undergoing transcriptional arrest, Cell 121 (2005) 913–923.
[35] T.A. Soucy, P.G. Smith, M.A. Milhollen, A.J. Berger, J.M. Gavin, S. Adhikari, J. E. Brownell, K.E. Burke, D.P. Cardin, S. Critchley, et al., An inhibitor of NEDD8-activating enzyme as a new approach to treat cancer, Nature 458 (2009) 732–736.
[36] L.M. Starita, A.A. Horwitz, M.C. Keogh, C. Ishioka, J.D. Parvin, N. Chiba, BRCA1/BARD1 ubiquitinate phosphorylated RNA polymerase II, J. Biol. Chem. 280 (2005) 24498–24505.
[37] A. Tufegdzic Vidakovic, M. Harreman, A.B. Dirac-Svejstrup, S. Boeing, A. Roy, V. Encheva, M. Neumann, M. Wilson, A.P. Snijders, J.Q. Svejstrup, Analysis of RNA polymerase II ubiquitylation and proteasomal degradation, Methods 159–160 (2019) 146–156.
[38] A. Tufegdzic Vidakovic, R. Mitter, G.P. Kelly, M. Neumann, M. Harreman, M. Rodriguez-Martinez, A. Herlihy, J.C. Weems, S. Boeing, V. Encheva, et al., Regulation of the RNAPII Pool Is Integral to the DNA Damage Response, Cell 180 (1245–1261) (2020), e1221.
[39] R. Verma, R. Oania, R. Fang, G.T. Smith, R.J. Deshaies, Cdc48/p97 mediates UV-dependent turnover of RNA Pol II, Mol. Cell 41 (2011) 82–92.
[40] J.C. Weems, B.D. Slaughter, J.R. Unruh, S. Boeing, S.M. Hall, M.B. McLaird, T. Yasukawa, T. Aso, J.Q. Svejstrup, J.W. Conaway, et al., Cockayne syndrome B protein regulates recruitment of the Elongin A ubiquitin ligase to sites of DNA damage, J. Biol. Chem. 292 (2017) 6431–6437.
[41] J.C. Weems, B.D. Slaughter, J.R. Unruh, S.M. Hall, M.B. McLaird, J.M. Gilmore, M. P. Washburn, L. Florens, T. Yasukawa, T. Aso, et al., Assembly of the elongin A ubiquitin ligase is regulated by genotoxic and other stresses, J. Biol. Chem. 290 (2015) 15030–15041.
[42] M.D. Wilson, M. Harreman, J.Q. Svejstrup, Ubiquitylation and degradation of elongating RNA polymerase II: the last resort, Biochim Biophys. Acta 1829 (2013) 151–157.
[43] M.D. Wilson, M. Harreman, M. Taschner, J. Reid, J. Walker, H. Erdjument-Bromage, P. Tempst, J.Q. Svejstrup, Proteasome-mediated processing of Def1, a critical step in the cellular response to transcription stress, Cell 154 (2013) 983–995.
[44] E.C. Woudstra, C. Gilbert, J. Fellows, L. Jansen, J. Brouwer, H. Erdjument-Bromage, P. Tempst, J.Q. Svejstrup, A Rad26-Def1 complex coordinates repair and RNA pol II proteolysis in response to DNA damage, Nature 415 (2002) 929–933.
[45] T. Yasukawa, T. Kamura, S. Kitajima, R.C. Conaway, J.W. Conaway, T. Aso, Mammalian Elongin A complex mediates DNA-damage-induced ubiquitylation and degradation of Rpb1, Embo J. 27 (2008) 3256–3266.
[46] T. Ye, J. Xu, L. Du, W. Mo, Y. Liang, J. Xia, Downregulation of UBAP2L inhibits the epithelial-mesenchymal transition via SNAIL1 regulation in hepatocellular carcinoma cells, Cell Physiol. Biochem. 41 (2017) 1584–1595.
[47] J.Y. Youn, W.H. Dunham, S.J. Hong, J.D.R. Knight, M. Bashkurov, G.I. Chen, H. Bagci, B. Rathod, G. MacLeod, S.W.M. Eng, et al., High-density proximity mapping reveals the subcellular organization of mRNA-associated granules and bodies, Mol. Cell 69 (517–532) (2018), e511.
[48] D. Zatreanu, Z. Han, R. Mitter, E. Tumini, H. Williams, L. Gregersen, A.B. Dirac-Svejstrup, S. Roma, A. Stewart, A. Aguilera, et al., Elongation factor TFIIS prevents transcription stress and R-loop accumulation to maintain genome stability, Mol. Cell (2019).